Clays and Clay Minerals, Vol. 51, No. 3, 264–278, 2003.

STRUCTURAL TRANSFORMATIONS OF CLAY MINERALS IN SOILS OF A CLIMOSEQUENCE IN AN ITALIAN ALPINE ENVIRONMENT

ALDO MIRABELLA[1,*] AND MARKUS EGLI[2]

[1] Istituto Sperimentale per lo Studio e la Difesa del Suolo, Piazza D'Azeglio 30, 50121 Firenze, Italy
[2] Department of Physical Geography, University of Zürich, Winterthurerstrasse 190, 8057 Zürich, Switzerland

Abstract—Clays of a soil sequence with five profiles in the Val Genova (northern Italy) along an elevation gradient with climate ranging from moderate to Alpine were investigated with XRD using several diagnostic treatments. Smectites developed in the surface horizons of podzolic soils either from chlorite through the removal of hydroxy interlayers or from mica, which weathers in a first step to regularly or irregularly interstratified clay minerals. Citrate treatment allowed the detection of low-charge expandable minerals in the Bhs or Bs horizons. Therefore, the reduction of the charge of 2:1 clay minerals occurred before the removal of hydroxy polymers by fulvic acids and low-weight organic acids. Due to the more intense podzolization process near the tree line, the d_{060} region showed a temporal evolution of trioctahedral to dioctahedral mineral structures in the well developed Podzols. The pedogenic smectites of the E or Bhs horizons generally included one or several populations with various charges. In most cases, smectite was a heterogeneous mixture of montmorillonite and interstratified beidellite-montmorillonite . A pure beidellite phase could not be detected. The soils near the tree line, where weathering processes were most intense, had two main components: one with a charge >0.75, representing vermiculite-like minerals, and the other with a charge near 0.25, representing smectite. The charges of the beidellitic component and montmorillonite were almost equal. The higher the weathering state of the investigated soils, the lower was the layer charge of smectites.

Key Words—Alpine Soils, Beidellite, Climosequence, Layer Charge, Montmorillonite, Podzol, Smectite, Weathering.

INTRODUCTION

A recent review reported the major mechanisms involved in podzolization and included the production of fulvic and low molecular weight organic acids that form soluble complexes with Al and Fe (Lundström *et al.*, 2000a,b).

Regarding the weathering of clay minerals, their sequence in podzolic soils is well established (Ross, 1980; Wilson, 1986). Such a sequence is characterized by the presence of chlorite and hydroxy-interlayered 2:1 clay minerals in the deep illuvial horizons and by the decrease or the disappearance of such minerals with the appearance of either vermiculite or smectite in the surface E horizon. Hereafter, hydroxy-interlayered 2:1 clay minerals will be referred to as HIV or HIS based on their layer charge. Recent work on both Podzols and associated Dystrochrepts in European Alpine environments has often reported the presence of smectite components in surface horizons (Righi and Meunier, 1991; Righi *et al.*, 1993; Carnicelli *et al.*, 1997; Mirabella and Sartori, 1998; Egli *et al.*, 2001a,b).

According to Righi *et al.* (1999) and Melkerud *et al.* (2000), smectites are the end-product of mica alteration in strongly leached and acidified E horizons of podzols. Furthermore, the study of Carnicelli *et al.* (1997) also demonstrated that chlorite can transform into a low-charge expandable mineral.

Ross (1980) reported that smectites in Spodosols showed some properties usually associated with vermiculites, this being due either to a relatively high layer charge and/or to concentration of the charge in the tetrahedral sheets. He also proposed that the absence of chlorite in E horizons of Spodosols was due to its destruction and demonstrated by laboratory weathering experiments that dioctahedral smectites could form from chlorites through the removal of hydroxy interlayers and the reduction of the layer charge. Successive laboratory experiments further confirmed this finding (Senkayi *et al.*, 1981).

The formation of smectite, or ethylene glycol (EG) expandable vermiculite, by the removal of hydroxy polymers from hydroxy-interlayered minerals (HIM) which originated from pedogenic intercalation of pre-existing expandable phyllosilicates, was reported by Malcolm *et al.* (1969) and April *et al.* (1986). The latter authors also suggested an alternative hypothesis: HIM minerals might never have formed in the surface horizons of the Spodosols they studied, where the presence of organic acids would hinder Al deposition.

Mass balance calculations on soils formed on granitic glacial till in Swiss Alpine environments indicate that extensive mineral weathering resulted in significant leaching losses of Si, major base cations, and Al (particularly from upper horizons). The greatest changes in soil chemistry occurred mostly in the early stages of

* E-mail address of corresponding author:
aldo.mirabella@issds .it
DOI: 10.1346/CCMN.2003.0510303

soil formation (Egli *et al.*, 2001a). Smectite and interstratified mica-smectite could be found in the most weathered horizons. The origin of smectite could be traced back to both chlorite and mica, which supports the fact that smectite is the end-product of chlorite alteration and illite-smectite, or even smectite, the end-product of mica weathering in strongly leached and acidified horizons (Egli *et al.*, 2001b). Gillot *et al.* (2000) used a chronosequence (6500–9850 y BP) to show that expandable phyllosilicates (vermiculites, smectites) are formed in the eluvial E horizon of Podzols in a short time (6500 y). The chemical composition of individual particles indicated that expandable phyllosilicates from the E horizon of Podzols were heterogeneous, involving a mixture of vermiculite, Mg-bearing smectites, and aluminous beidellite (Gillot *et al.*, 2000).

A mineralogical investigation along a soil climosequence in an Alpine valley in Trentino (Italy) showed that in the surface horizon, all the soils, except that developing at the lowest elevation, contained an expandable clay mineral, formed through the removal of the hydroxy interlayers from chlorite or chlorite-vermiculite intergrades (Mirabella and Sartori, 1998).

In the present study, the climosequence was investigated to obtain more detailed information on the structural transformation of clay minerals in response to the climate and on the effect of hydroxy polymers on the expandable properties of low-charge clay minerals.

STUDY AREA

A sequence of five soil profiles in the Val Genova (northern Italy; Figure 1) along an elevation gradient ranging from 950 up to 2440 m above sea level (a.s.l.) was investigated (Table 1). The soil profiles were selected from an existing soil cartography study and soil inventory (Sartori and Mancabelli, 2002). The soil profiles are assumed to be representative of the elevation zones. The soils vary from Umbric Regosol to Haplic Podzols (Tables 1 and 2), according to the FAO-UNESCO classification (1990). All soils were developed on tonalitic-granodioritic till. During the last glaciation period, all of the sites investigated here were covered by ice. Alpine glaciers have varied over the last 12,000 y near the borders of the moraines dating from 1850 ('little ice age'). Due to the position of the investigation site in the landscape and according to the geomorphological study of Baroni and Carton (1990), soil ages vary between 12,000 and 16,000 y.

It can be assumed that climate was more or less stable during soil formation (Egli *et al.*, 2003). Due to the small differences in the soil age, the similar geology, and stable climatic conditions, the changes in the weathering processes in the soils can be attributed primarily to the climate factor. Present climatic conditions for Pinzolo, a nearby village at 776 m a.s.l., are +8.7ºC mean annual temperature and 1100 mm mean annual precipitation (mean values on the basis of 20 y of observation). At the nearby meteorological station of M.ga Bissina at 1792 m

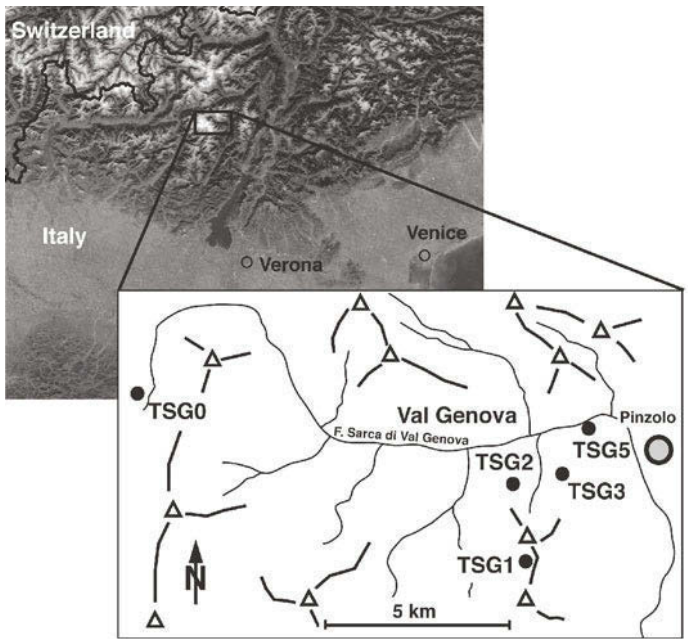

Figure 1. Location (data source: satellite image 'Terra'; Jacques Descloitres, MODIS Land Rapid Response Team, NASA/GSFC) and schematic map of Val Genova and of the investigation sites TSG0–5. Triangles indicate summits and the bold lines refer to ridges.

https://doi.org/10.1346/CCMN.2003.0510303 Published online by Cambridge University Press

Table 1. Characteristics of the study sites.

Profile	Location	Elevation (m)	Aspect (ºN)	Parent material	Vegetation[1]	FAO-UNESCO Legend (1990)	Form of humus
TSG0	Lobbia Alta	2440	100	Granodiorite-rich till	*Caricetum curvulae*	Umbric Leptosol	Dysmoder
TSG1	Spadalone	2170	340	Granodiorite-rich till	*Rhododendro ferruginei-vaccinietum*	Cambic Podzol	Eumoder
TSG2	Malga S. Giuliano	1830	40	Granodiorite-rich reworked till	*Larici-Piceetum*	Haplic Podzol	Dysmoder
TSG3	Malga Campo	1660	115	Granodiorite-rich reworked till	*Larici-Piceetum*	Haplic Podzol	Dysmoder
TSG5	Cascate Nardis	950	20	Tonalite till	*Picea abies* and *Abies alba*	Spodo-Dystric Cambisol	Dysmoder

[1] classification system according to Keller *et al*. (1998) and Pedrotti (1993)

a.s.l., the mean annual temperature is 4.3ºC and the mean annual precipitation is 1436 mm. At the Carlo Magno station at 1681 m a.s.l. and at the Grostè station at 2505 m a.s.l., the mean annual temperatures are 3.9ºC and −0.4ºC, respectively.

MATERIALS AND METHODS

Soil material was collected from excavated profile pits. Soil pH (in water and in 1 N KCl) was determined on air-dried samples using a soil:solution ratio of 1:2.5.

Table 2. Some chemical characteristics of the investigated soils.

Horizon	pH H_2O	pH KCl	C (%)	N (%)	Fe(o)[1] (%)	Al(o)[1] (%)
Profile TSG0						
A	5.3	4.5	5.0	0.18	0.13	n.d.
AC	5.7	4.6	1.4	0.06	0.16	n.d.
Profile TSG1						
AE	4.8	4.0	7.0	0.26	0.69	n.d.
A2	5.1	4.3	4.5	0.26	0.94	0.93
Bhs	4.9	4.3	9.2	0.30	1.35	2.40
Profile TSG2						
E	n.d.	n.d.	7.7	0.38	0.74	0.33
Bhs	4.9	4.1	10.1	0.47	1.88	2.20
Bs	4.8	4.4	9.2	0.33	0.78	3.06
BC	5.1	4.6	4.0	0.13	0.30	2.28
Profile TSG3						
AE	3.8	3.1	11.5	0.69	0.50	0.29
Bhs	4.6	n.d.	11.1	0.60	1.93	1.72
Bs1	4.9	4.3	13.8	0.48	1.10	3.12
Bs2	5.1	4.3	12.3	0.38	1.95	2.91
Profile TSG5						
AE	5.0	4.3	9.8	0.49	0.84	1.50
Bs1	5.2	4.5	5.2	0.25	0.86	1.83
Bs2	5.3	4.6	3.4	0.12	0.75	1.76
BC	5.6	4.8	2.2	0.10	0.42	1.83

[1]oxalate-extractable Fe or Al
n.d. not determined

Total C and N contents were determined by the Walkley-Black and the Kjeldahl methods, respectively. In addition, the oxalate-extractable fractions were measured for the elements Fe and Al. Element pools in the soil (Ca, Mg, K, Na, Fe, Al, Mn, Si, Ti, Zr and V) were determined by a method of total disintegration. Oven-dried (70ºC) samples were dissolved using a mixture of HF, HCl, HNO_3 and H_3BO_3. Concentrations of Ca, Mg, K, Na, Fe, Mn, Al, Si, Ti, Zr and V were determined by atomic absorption spectroscopy, in part using a graphite furnace.

The clay fraction (<2 μm) was obtained by dispersion with Calgon and sedimentation in water. Specimens were then Mg saturated, washed free of chlorides and freeze dried. Clay-aggregate samples, oriented on glass slides from a water suspension, were analyzed with a 3 kW Rigaku D/MAX III C diffractometer, equipped with a horizontal goniometer, a curved-beam graphite monochromator and Cu radiation. Slides were step-scanned from 2 to 15º2θ with steps of 0.02º2θ at 2 s intervals. The following treatments were performed: Mg saturation, ethylene glycol solvation and K saturation, followed by heating for 2 h at 335ºC and 550ºC. The heat treatment at 335ºC allows the distinction between chlorite and HIV (hydroxy-interlayered vermiculite). Prior to these treatments, amorphous Al and Fe phases were dissolved using an oxalate extraction in samples from the Bs and BC horizon of profile TSG2 and from the Bs1 and Bs2 horizons of profile TSG3. When chlorite was present, the presence of kaolinite was checked using infrared analysis (OH-stretching region near 3690 cm^{-1}). The 060 region was studied using XRD on random mounts prepared by back-filling Al holders and gently pressing filter paper on top and then step-scanned from 58 to 64º2θ with steps of 0.02º2θ at 10 s intervals. Diffraction patterns were smoothed by a Fourier transform function and fitted by the Origin™ PFM using the Pearson VII algorithm. Background values were calculated by means of a non-linear function (polynomial 2nd order function; Lanson, 1997).

https://doi.org/10.1346/CCMN.2003.0510303 Published online by Cambridge University Press

Table 3. Geochemical characteristics (total contents) of the fine earth (<2 mm) and soil skeleton (>2 mm) of the parent material of the individual sites.

Site and soil depth	Org. matter* (%)	Al_2O_3 (%)	SiO_2 (%)	TiO_2 (%)	CaO (%)	MgO (%)	K_2O (%)	Na_2O (%)	Fe_2O_3 (%)	MnO_2 (%)	VOOH (%)
TSG0											
fine earth	0.82	14.49	72.1	0.60	4.45	0.84	1.38	2.73	1.84	0.045	0.0107
soil skeleton	0.14	16.14	65.9	1.14	4.34	1.68	2.55	2.70	4.23	0.099	0.0081
TSG1											
fine earth	0.88	14.62	67.5	1.13	2.62	2.23	1.94	3.15	4.90	0.144	0.0287
soil skeleton	0.00	16.25	69.1	0.63	3.63	1.18	2.10	3.92	2.65	0.094	0.0072
TSG2											
fine earth	0.98	15.73	71.4	0.50	2.60	0.72	1.44	3.78	1.82	0.058	0.0203
soil skeleton	0.00	16.20	70.4	0.45	3.20	0.89	1.77	3.92	2.65	0.066	0.0047
TSG3											
fine earth	0.00	15.99	68.9	0.95	2.98	1.52	1.96	3.25	3.46	0.112	0.0223
soil skeleton	0.00	17.19	69.4	0.50	3.53	0.89	1.70	4.18	2.07	0.072	0.0051
TSG5											
fine earth	0.00	16.51	68.8	1.37	1.82	1.78	2.05	1.79	5.27	0.090	0.0183
soil skeleton	0.00	15.29	67.9	0.87	3.98	1.74	2.52	2.65	4.38	0.105	0.0092

* calculated as org. C × 1.72

Sodium citrate treatment was performed to extract hydroxy Al (or Fe) contaminants from the interlayers of 2:1 clay minerals. The Tamura procedure (1958) was applied in a modified form, in which a contact time of 24 h without extractant removal was obtained by heating the samples in an autoclave at 135ºC. The Na citrate-treated clays were Mg saturated, solvated with ethylene glycol, K saturated and heated at 335ºC and 550ºC for 2 h. The XRD patterns of the treated samples were then compared with those of the corresponding untreated ones.

Layer-charge estimation of smectites was performed using the long-chain alkylammonium ion C18 according to the method proposed by Olis *et al.* (1990).

For the monolayer to bilayer transition, equation 1 was used:

$$d_{001} = 8.21 + 34.22\text{MLC} \quad (1)$$

where MLC = mean layer charge and *d* values are given in Å.

For the bilayer to pseudotrimolecular layer transition, the equation is:

$$d_{001} = 8.71 + 29.65\text{MLC} \quad (2)$$

To distinguish beidellitic from montmorillonitic smectites, the clay fraction from untreated samples was Li saturated, heated at 300ºC overnight and then glycerol solvated (Greene-Kelly, 1953). To avoid the effects of the reaction of the clay film with Na from the glass slide when it is heated at 300ºC, the Li-saturated clay was heated in a platinum crucible. The sample was then resuspended in water and oriented on a glass slide. Long-chain alkylammonium ion (C18) was also applied to the Li-saturated and heated clays to determine the charge of beidellitic components.

RESULTS

Chemical analyses

All the soils are acid, with the lowest pH values being found in the Cambic Podzol, profile TSG1, and in the two Haplic Podzols, profiles TSG2 and TSG3 (Table 2). The three Podzols show the characteristic eluvial features with an increase of the amount of organic C and oxalate-extractable forms of Al and Fe in the B horizons. No clear translocation of organic C or Fe and Al was discernible in the soils TSG0 and TSG5 (Table 2). All soils developed from the same parent material as shown by the total chemical analysis in Table 3.

Clay mineral analyses

Profile TSG0 (Umbric Leptosol), developing at 2440 m, showed in the surface A horizon the presence of a small amount of smectite with a *d* value of 1.63 nm following ethylene glycol solvation (Figure 2). The slightly lower value of the *d* spacing of this expandable mineral could indicate some interstratification. This smectitic component may derive from the weathering of mica or from chlorite (Carnicelli *et al.*, 1997; Egli *et al.*, 2001b), both these minerals being present in the soil. Kaolinite, vermiculite, hydroxy-interlayered vermiculite (HIV) and a random interstratified mica-HIV mineral were also detected in this profile. In fact, HIV did not collapse to 1.0 nm after K saturation, but only after the heating treatment at 335ºC (data not shown). The irregularly interstratified mica-HIV, denoted by the peak at 1.25 nm in the EG-solvated sample (Figure 2) maintained this position after K saturation and shifted towards 1.0 nm after heating at 335ºC. The smectitic component was absent in the AC horizon below, while

https://doi.org/10.1346/CCMN.2003.0510303 Published online by Cambridge University Press

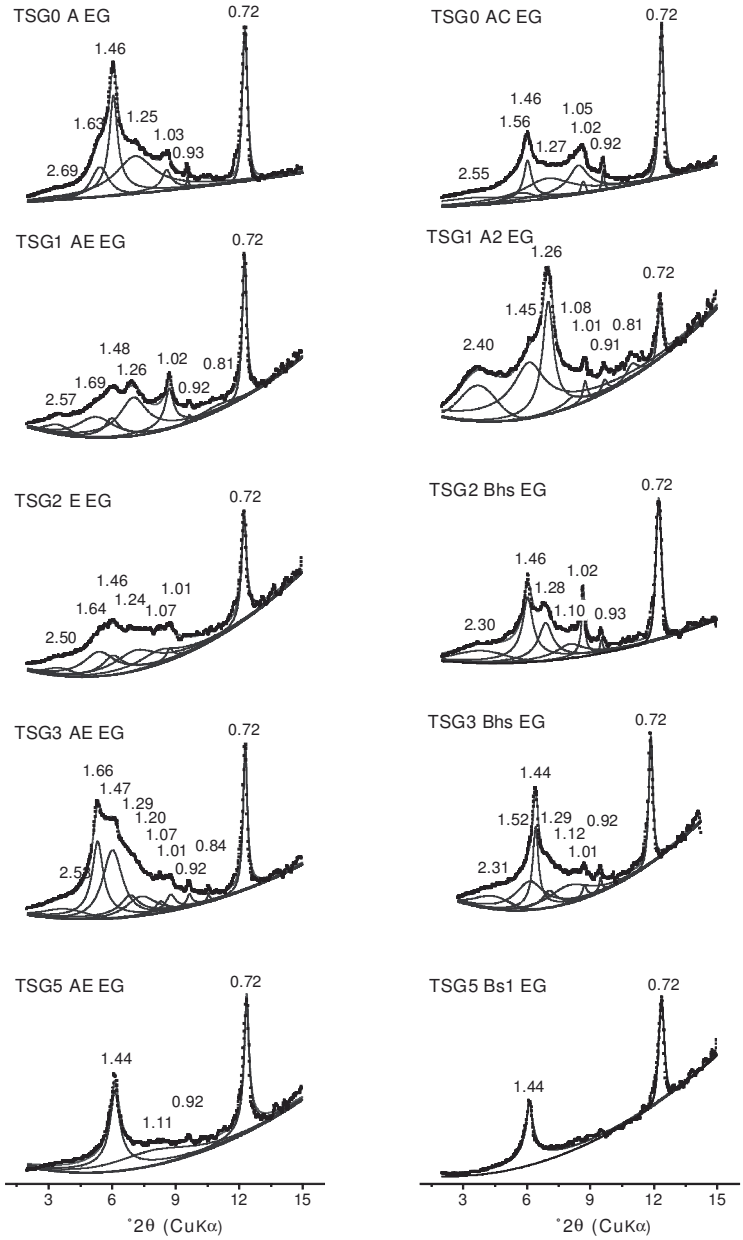

Figure 2. XRD patterns of ethylene glycol (EG)-solvated soil clays (<2 μm) surface (A, AE or E horizons) and subsoil (AC, A2, Bhs or Bs horizon) samples. The XRD curves are corrected for Lorentz and polarization factors. *d* values are given in nm.

mica, vermiculite, HIV, the irregularly interstratified mica-HIV mineral and chlorite were present (XRD patterns not shown).

Soil profile TSG1, a Cambic Podzol, developing at 2170 m, just above the tree line, already had a higher proportion of smectite in the surface AE horizon (Figure 2). Mica, kaolinite and a regularly interstratified mica-vermiculite mineral (hydrobiotite) (d_{001} and d_{002} spacings at 2.57 and 1.26 nm, respectively) were also present. In the underlying A2 horizon, the interstratified mica-vermiculite mineral became the predominant clay mineral. Chlorite was only detectable in the Bhs horizon, whereas no smectite could be detected in the lower soil horizons. Furthermore, vermiculite decreased with soil depth, while HIV, which collapsed to 1.0 nm after heating at 550ºC, and mica increased.

The surface E horizon of profile TSG2, a Haplic Podzol developing at 1830 m a.s.l., just below the tree line, had almost equal amounts of an expandable clay mineral and vermiculite (Figure 2). In this horizon, a regularly interstratified mica-vermiculite mineral, with peaks at 2.5 and 1.26 nm, mica and kaolinite were also present, while HIV was absent (Figure 3). HIV, the regularly interstratified mica-HIV and a small amount of

https://doi.org/10.1346/CCMN.2003.0510303 Published online by Cambridge University Press

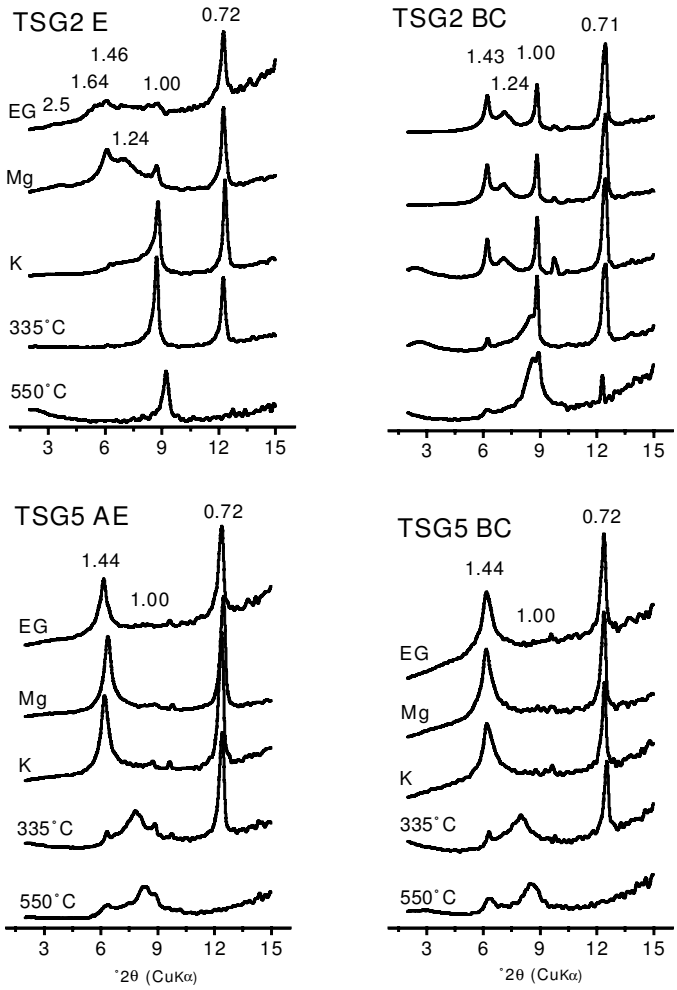

Figure 3. XRD patterns of soil clays (<2 μm) of some selected samples. The XRD curves are smoothed and corrected for Lorentz and polarization factors. *d* spacings are given in nm. Mg = Mg saturation, EG = ethylene-glycol solvation, K = K saturation and corresponding heating treatments.

vermiculite were detected in the underlying Bhs horizon. The clay mineralogy of the Bs horizon was similar to that of the Bhs horizon, while the BC horizon differed only in the presence of a discernible peak of chlorite (Figure 3).

The surface AE horizon of profile TSG3, a Haplic Podzol at 1660 m, contained a similar amount of smectite to that detected in the surface E horizon of soil TSG2 (Figure 2). Vermiculite, HIV, interstratified mica-HIV, kaolinite and traces of mica were also identified in this horizon. The amount of the regularly interstratified mica-HIV and vermiculite decreased in the lower Bhs and Bs horizons, while, correspondingly, the HIV mineral increased. Traces of chlorite were detected in both the Bs and BC horizons.

No smectite or vermiculite could be identified in profile TSG5, a Dystric Cambisol developing at 940 m (Figure 3). The dominant 2:1 clay mineral was HIV, denoted by the peak at 1.4 nm in the EG-solvated and Mg-saturated samples. This peak remained unchanged after K saturation and shifted towards 1.0 nm after heating at 335ºC. Chlorite, characterized by the peak at 1.44 nm in the samples heated at 550ºC, was present throughout the profile and increased with depth. Kaolinite and traces of mica were the other clay minerals present. This soil showed no trace of vermiculite, due to the failure of the 1.44 nm peak to collapse to 1.0 nm after K saturation. Unlike the other soils examined, 2:1 clay minerals were also completely Al interlayered in the surface A horizon.

Citrate treatment of the clay fraction

This treatment, which is able to remove Al and Fe polymers from the interlayers of clay minerals, induced significant changes in the XRD patterns of all soils. The surface A horizon of soil TSG0 showed a better resolved peak around 1.71 nm in the ethylene glycol-solvated sample, which was assigned to smectite (Figure 4). Furthermore, the citrate was able to almost completely remove the polymers from the interlayers of 2:1 clay

https://doi.org/10.1346/CCMN.2003.0510303 Published online by Cambridge University Press

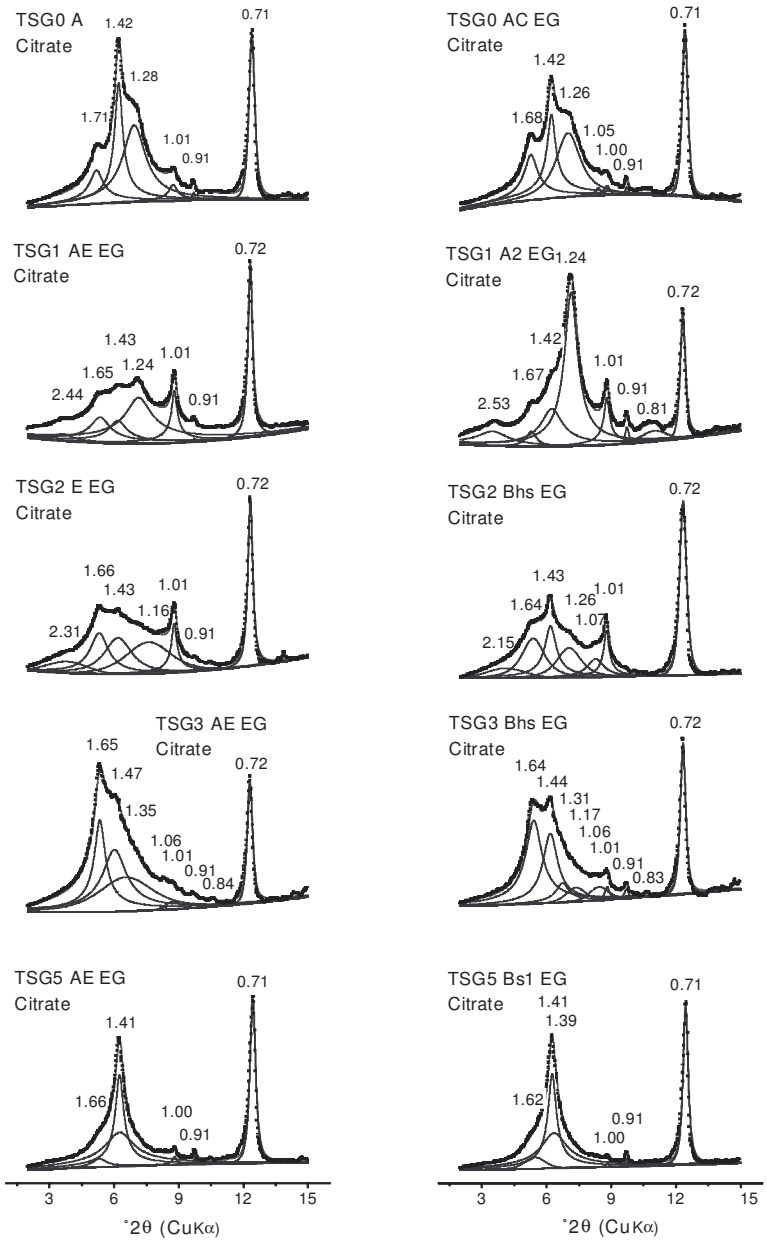

Figure 4. XRD patterns of soil clays (<2 μm) from the investigated sites. Clays were treated with Na citrate and solvated with ethylene glycol (EG). The XRD curves are corrected for Lorentz and polarization factors. *d* values are given in nm.

minerals, as indicated by the shifting to 1.0 nm of the peak at 1.4 nm following K saturation (data not shown). In the untreated sample, this peak collapsed to 1.0 nm only after heating at 335ºC. Also, the irregularly interstratified mica-HIV mineral transformed into an irregularly interstratified mica-vermiculite mineral after the citrate treatment. The changes in the deeper AC horizon were even more evident. In the EG-solvated sample, a smectitic component was clearly discernible at 1.68 nm (Figure 4), as well as an irregularly interstratified mica-vermiculite mineral at 1.26 nm, which collapsed to 1.0 nm following K saturation.

The main changes in the soil profile TSG1 were detected in the lower horizons (A2 and Bhs). The main modification in the AE horizon was due to the transformation of the irregularly interstratified mica-HIV into an irregularly interstratifed mica-vermiculite, which collapsed to 1.0 nm after K saturation (data not shown). The citrate treatment completely freed the interlayers of vermiculitic components, as evidenced by their basal dimension of 1.0 nm after K saturation. Both the A2 and Bhs horizons (Figure 4) showed a distinct peak around 1.67 nm after EG solvation. This expandable mineral could not be detected in the X-ray

https://doi.org/10.1346/CCMN.2003.0510303 Published online by Cambridge University Press

patterns of the untreated samples. Furthermore, K saturation was more effective in producing a shift towards 1.0 nm of the peaks belonging to 2:1 clay minerals in the sample of the Bhs horizon.

The citrate treatment revealed a larger amount of smectite in the surface AE horizon of soil TSG2, as shown by the integral intensity of the peak at 1.65 nm in the EG-solvated samples (Figures 2 and 4). This expandable mineral could also be clearly detected in the lower Bhs horizon (Figure 4), while traces were also found in the Bs and BC horizons (Figure 5). All these horizons contained mainly vermiculite, whereas the irregularly interstratified mica-vermiculite and mica-HIV coexist in the Bs and BC horizons. Mica-vermiculite and mica-HIV were characterized in the Mg-saturated sample by the peak at 1.24 nm which collapsed to 1.0 nm after K saturation and heating at 335ºC (Figure 5).

The surface horizon of soil TSG3 did not show a significant difference after citrate treatment as regards the smectitic component (Figures 2 and 4); in fact, the untreated sample already contained a large amount of smectite. Vermiculite now appears almost completely free of hydroxy polymers, as indicated by the shift of the 1.4 nm peak towards 1.0 nm after K saturation (data not shown). A shoulder towards lower angles in the 1.0 nm peak showed the presence of some residual polymers in the interlayers of vermiculite (Barnhisel and Bertsch, 1989). Citrate treatment noticeably affected XRD patterns of the lower Bhs horizon, where a smectite peak, equally intense as that of vermiculite, appeared at ~1.65 nm in the EG-solvated sample (Figure 4). Some residual hydroxy polymers were also present in the interlayer space of vermiculite. The citrate-treated samples of the Bs1 and Bs2 horizons contained mostly vermiculite. In the untreated samples of the same

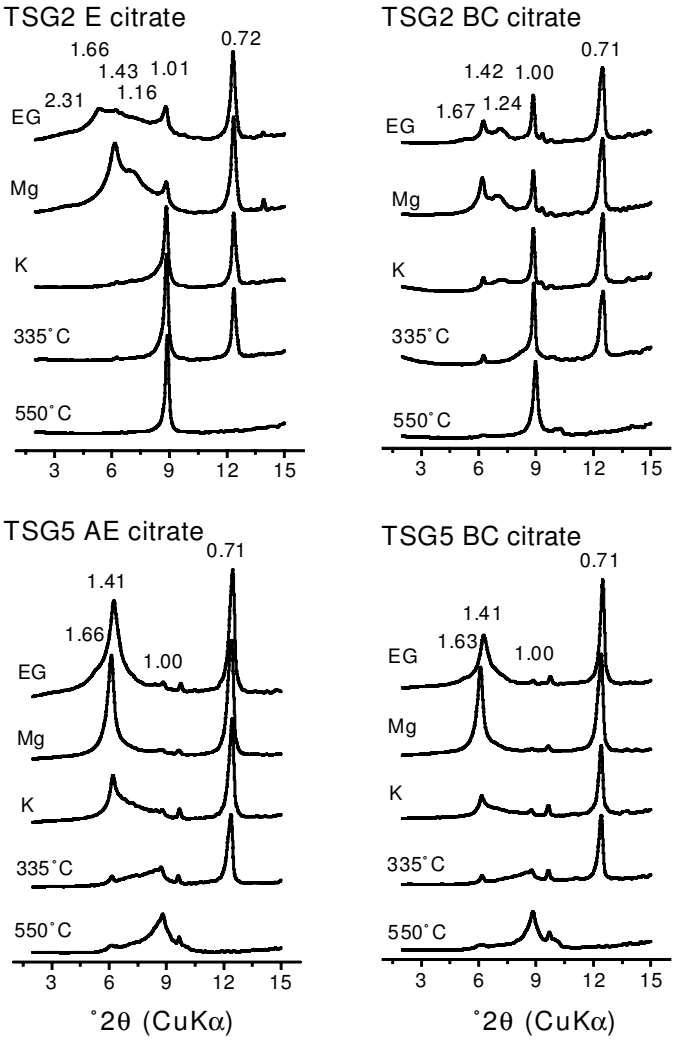

Figure 5. XRD patterns of soil clays (<2 μm) of some selected samples treated with Na citrate. The XRD curves are smoothed and corrected for Lorentz and polarization factors. *d* spacings are given in nm. Mg = Mg saturation, EG = ethylene-glycol solvation, K = K saturation and corresponding heating treatments.

https://doi.org/10.1346/CCMN.2003.0510303 Published online by Cambridge University Press

horizons, the dominant component was an HIV and some interstratified mica-HIV.

A shoulder towards low angles in the peak around 1.45 nm of the citrate-treated EG-solvated sample from the surface AE horizon of soil TSG5 indicated the presence of a low-charge expandable mineral (Figure 4). This shoulder was also present in the lower horizons, but its intensity decreased with depth. With regard to vermiculite, the citrate treatment was able to remove only a part of the interlayer polymers in this soil, as indicated by the persistence of a peak around 1.4 nm in the XRD pattern of the K-saturated samples (Figure 5).

Trioctahedral vs. dioctahedral transformation

The investigation of the d_{060} reflections showed that no substantial transformation from trioctahedral to dioctahedral minerals has taken place from the AC to the A horizon of soil TSG0. X-ray profile fitting of the samples of these two horizons enabled the separation of a quartz peak near 0.1543 nm and trioctahedral species at 0.1550 and 0.1539 nm which could be attributed to chlorite and biotite, respectively (Moore and Reynolds, 1997). A small peak was discernible at 0.1524 nm due to Fe-rich dioctahedral minerals (Fanning *et al*., 1989); the other dioctahedral species were represented by the peaks in the 0.1509–0.1491 nm region (Figure 6).

The dioctahedral species, in comparison to trioctahedral ones, were not present in large amounts in the lower Bhs horizon of soil TSG1. The latter decreased slightly towards the surface AE horizon (Figure 6). Also in this profile, dioctahedral Fe-rich minerals were represented by a peak around 0.1526 nm which decreased in the surface horizon.

The XRD pattern of the 060 region of the BC horizon of the TSG2 soil was characterized by two large peaks. The first was decomposed into two elementary peaks at 0.1543 and 0.1538 nm, attributed to quartz and trioctahedral minerals. The other was resolved into three elementary peaks: those at 0.1508 and 0.1502 nm were assigned to dioctahedral mineral species; whereas that at 0.1492 nm was assigned to kaolinite (Moore and Reynolds, 1997). The proportion of trioctahedral and dioctahedral minerals varied noticeably in the profile, with trioctahedral species decreasing progressively towards the soil surface (Figure 6). Soil TSG3 showed similar XRD patterns and the same trends in the change of trioctahedral to dioctahedral minerals approaching the surface of the soil. This evolution of clay minerals indicated a progressive shift from trioctahedral to dioctahedral structures with an increasing contribution of expandable dioctahedral minerals.

Soil TSG5 had a slightly higher proportion of trioctahedral minerals compared to dioctahedral species in the lower BC horizons. In this horizon, dioctahedral Fe-rich minerals are clearly discernible. Approaching the soil surface, the trioctahedral minerals tended to decrease in favor of dioctahedral ones (Figure 6).

Localization of the charge

Montmorillonite can be differentiated from beidellite and nontronite by its irreversible collapse after Li saturation and its lack of expandability after glycerol solvation (Greene-Kelly, 1953). This analysis was performed only with samples where smectite was present. The interpretation of the results can be difficult in those samples that exhibit, at the same time, the presence of vermiculite, irregularly interstratified mica with 2:1 minerals and HIV, whose peaks in the 1.4–1.0 nm region may interfere with the peak of smectite, especially when this mineral is present in small amounts.

The XRD patterns of the Li-saturated, heated at 300ºC, and then glycerol-solvated specimens are shown in Figure 7. The sample from the surface A horizon of TSG0 contains smectite, vermiculite, mica-HIV, mica and kaolinite. Lithium saturation and the subsequent heating process at 300ºC caused a partial shift of the peak at 1.42 nm towards 1.0 nm, overlapping the peak due to both vermiculite and mica; a very broad peak could be observed between the residual peak at 1.42 nm and the peak at 1.0 nm. The intensity of the peak at 1.42 nm increased slightly following glycerol solvation. This was indicative of a beidellitic phase in part interstratified with montmorillonite, because it failed to expand to 1.77 nm with glycerol. The peak at 1.0 nm could be assigned to irreversibly collapsed montmorillonite, vermiculite and mica. The presence of low-charge beidellitic and montmorillonitic species was, furthermore, checked with the C18 treatment before and after Li saturation and heating (see below). The surface AE horizon of soil TSG1 had similar properties. The Li saturation and heating at 300ºC produced a small increase of the mica peak at 1.0 nm which decreased slightly with the glycerol treatment, thus indicating the presence of both montmorillonite and beidellite. The beidellite component is interstratified with montmorillonite due to the partial XRD peak expansion up to 1.43 nm (Figure 7).

Lithium saturation of the clay sample from the surface E horizon of soil TSG2 caused a partial collapse to 1.22 nm of the peak at 1.42 nm in the XRD pattern of the Mg-saturated sample. The subsequent heating at 300ºC showed a noticeable increase of the peak at 1.01 nm and a decrease of the intensity of the peak at 1.22 nm. With glycerol solvation, an increase of the peak at 1.42 nm could be observed. Therefore, this sample contained montmorillonite and an interstratified beidellite-montmorillonite (Figure 7).

The Li saturation and glycerol solvation of the sample from the surface AE horizon of soil TSG3 indicated some montmorillonite and more interstratified beidellite-montmorillonite, than any of the other samples (Figure 7).

In most cases, the XRD patterns are typically those of mixed-layered minerals, indicating the heterogeneity of

https://doi.org/10.1346/CCMN.2003.0510303 Published online by Cambridge University Press

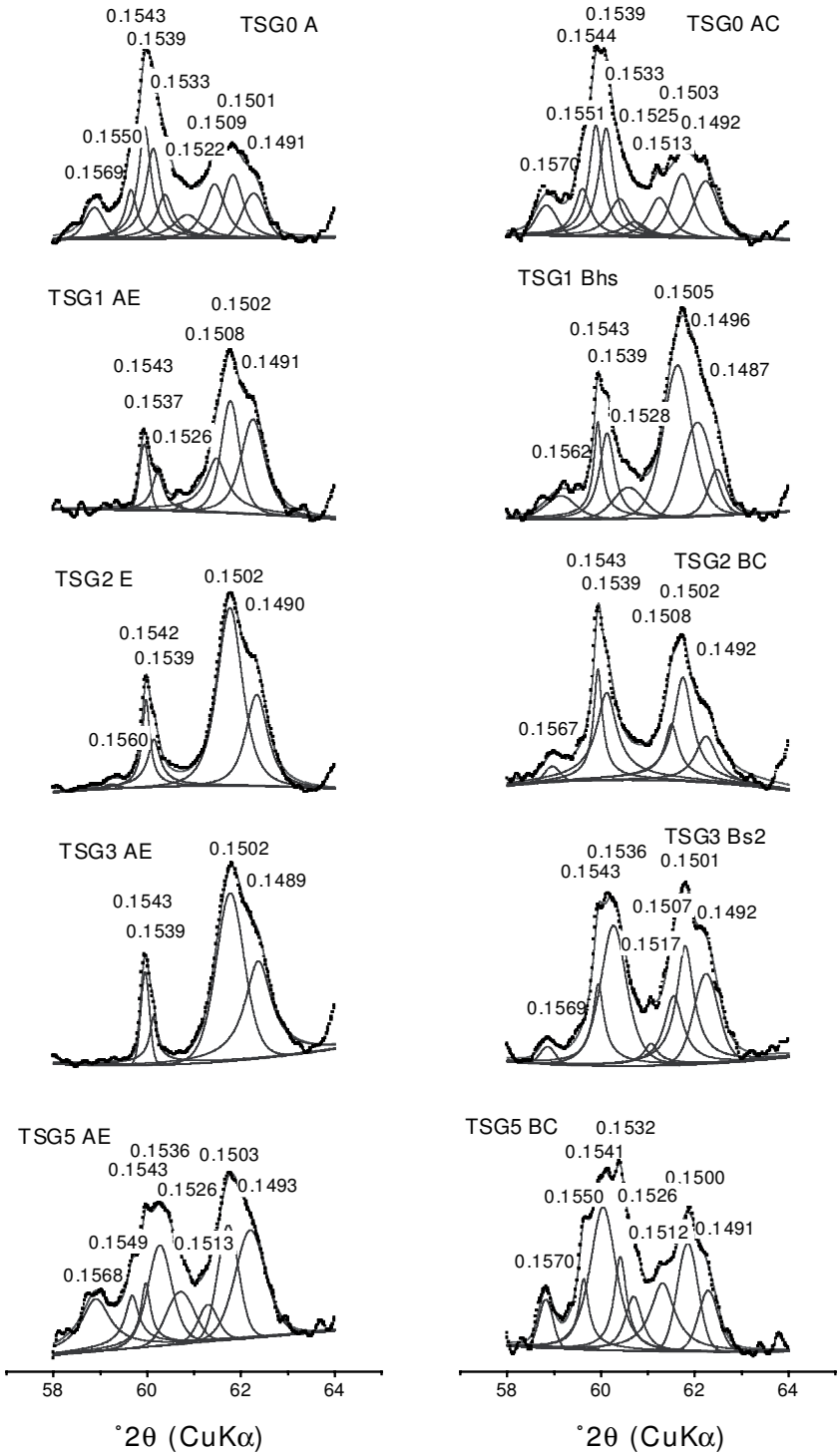

Figure 6. Deconvolution of XRD peaks in the d_{060} region of the surface and subsoil samples of the investigated sites. *d* values are given in nm. The dots represent the smoothed, measured data and the solid lines correspond to the individual peaks and the envelope curve.

the amount of charge. According to Petit *et al.* (2002), this heterogeneity can be effective not only from one particle to another, but also from one layer to another within the same particle.

Layer-charge estimation

Alkylammonium saturation. Deconvolution of the XRD pattern of the A horizon clay sample of soil TSG0, after long-chain alkylammonium ion C18 satura-

https://doi.org/10.1346/CCMN.2003.0510303 Published online by Cambridge University Press

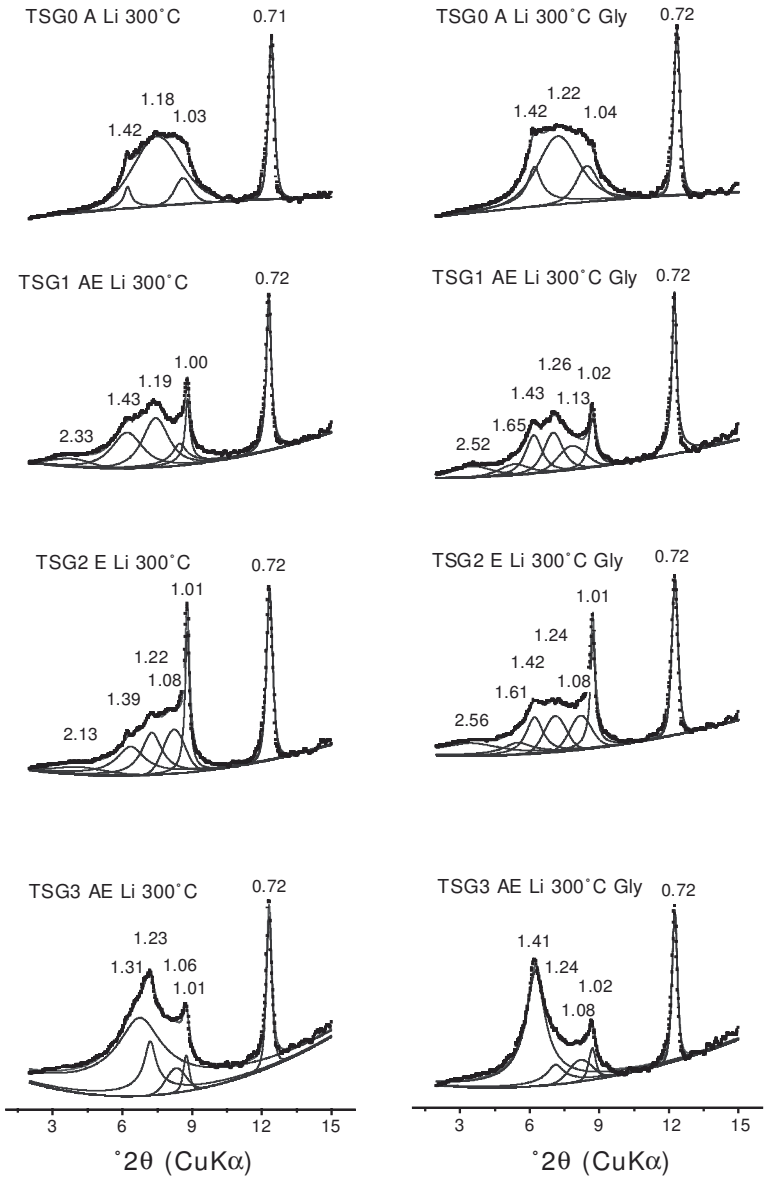

Figure 7. XRD patterns of soil clays treated with Li and heated at 300ºC. Re-expansion is measured by means of glycerol solvation (Greene-Kelly test). The XRD curves are corrected for Lorentz and polarization factors. *d* values are given in nm.

tion, gave a series of elementary curves with their maxima at 3.71, 2.10, 1.86, 1.57, 1.44, 1.23, 1.04 and 0.92 nm. In the low-angle region, which is relevant for the calculation of layer charge, two low-intensity peaks at 3.71 and 2.10 nm represent two distinct mineral species with total layer charge per half unit-cell (ξ) of 0.96 and 0.37, respectively, which could be assigned to a high-charge vermiculite and to a low-charge smectite (Figure 8). The value of 0.96 is, however, beyond the limits of the C-18 BTP regression model of Olis *et al.* (1990). Values of layer charges calculated from *d* spacings >3.1 nm are, therefore, indicated as >0.75. Another expandable mineral was denoted by a larger peak at 1.57 nm which indicates a total layer charge (ξ) of 0.22. Even though this value is below the limit for the evaluation of layer charge with the conventional alkylammonium ion-exchange technique (Lagaly, 1994), these low *d* values are consistent with the mono-to-bilayer (MTB) simple linear regression model, especially with the use of *n*C = 18 (Olis *et al.*, 1990).

The XRD pattern of the clay sample from the AE horizon of soil TSG1 was different from those discussed previously. The peak at 3.70 nm, belonging to a high-charge component and indicating a paraffin-type configuration and a mean layer charge of >0.75 per half unit-cell (ξ), is now more intense. The peak at 2.23 nm is also more intense and points to a low-charge component with a (ξ) of 0.41 per half unit-cell.

https://doi.org/10.1346/CCMN.2003.0510303 Published online by Cambridge University Press

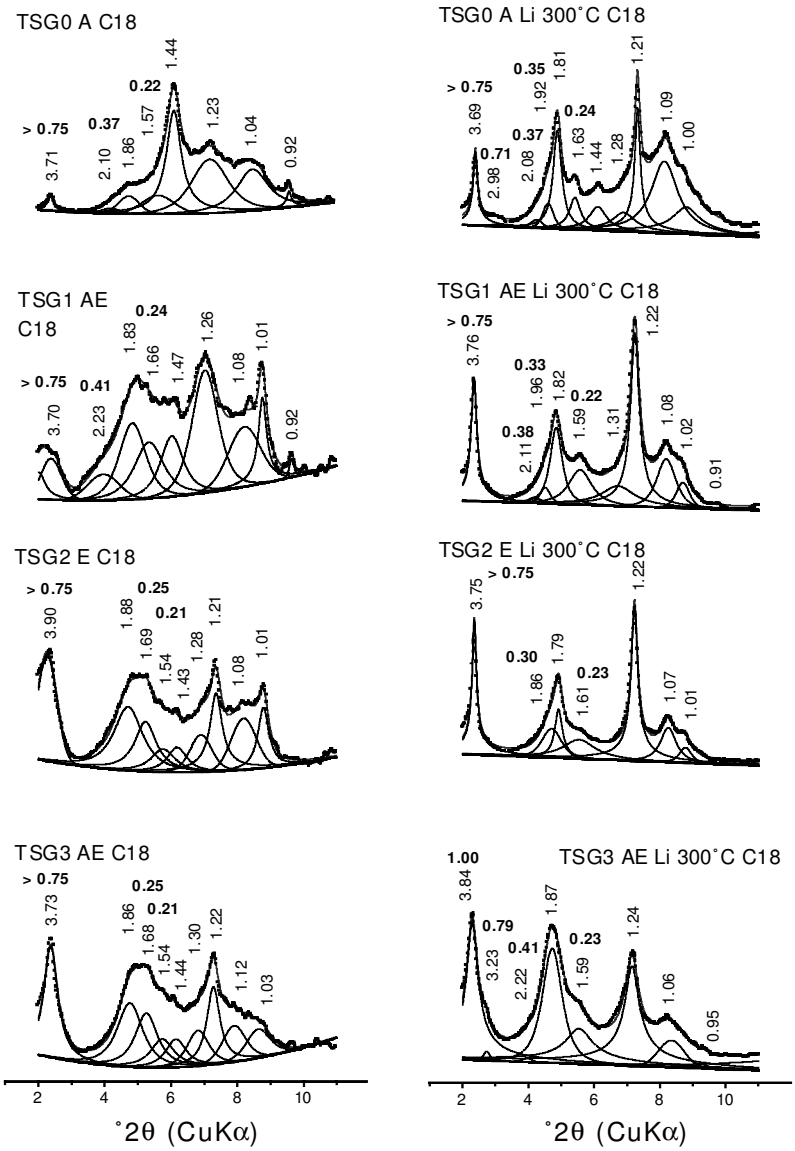

Figure 8. XRD patterns of soil clays (<2 μm) of the investigated sites. Clays were treated with C18 (18-alkylammonium ion) without or with Li saturation and heating at 300ºC. The XRD curves are corrected for Lorentz and polarization factors. *d* values are given in nm. The bold numbers indicate the calculated layer charge per half unit-cell.

The diffraction pattern of the surface E horizon of soil TSG2 was characterized by an intense peak at 3.90 nm, corresponding to a mineral component with a high mean layer charge (>0.75), while low-charge components are described by an intense peak at 1.69 nm and a lower one at 1.54, corresponding to 0.25 and 0.21 mean layer charges per half unit-cell, respectively. The K saturation caused an almost complete shift of the peak at 1.42 nm to 1.0 nm (Figure 3). The Li treatment allowed us to discern the montmorillonitic and beidellitic components that were characterized by a low charge (according to the C18 treatment). This suggests that K saturation is not a good tool for distinguishing between high- and low-charge expandable minerals.

Similarly, the sample from the surface AE horizon of soil TSG3 gave three different peaks centered at 3.73, 1.68 and 1.54 nm, corresponding to mean layer charges of >0.75, 0.25 and 0.21 per half unit-cell, respectively. The intensities of these peaks were comparable to those from the surface E horizon of soil TSG2. The result of the C18 saturation of the clay minerals from the surface A horizon of soil TSG5, developing at the lower altitude, was quite different. The high-charge mineral was represented in the XRD pattern by a peak at 3.77 nm, corresponding to a mean layer charge of >0.75, while the low-charge component was almost negligible and represented by a small and broad peak at 2.10 nm which corresponds to a mean layer charge of 0.41 per half unit-cell (data not shown).

https://doi.org/10.1346/CCMN.2003.0510303 Published online by Cambridge University Press

Li and alkylammonium saturation. The alkylammonium ion saturation, performed on Li-saturated and heated samples, allows the identification of the tetrahedral charge. When compared to the untreated samples, Li-treated clays gave slightly different XRD patterns (Figure 8). In general, the intensity of the peak of the high-charge component around 3.70 nm increases simultaneously with the corresponding decrease of that of the low-charge components. According to Olis *et al.* (1990), Li-saturated montmorillonite is in fact not affected by the alkylammonium ion saturation.

Residual peaks at 2.08, 1.92 and 1.63 nm in the Li-treated sample from the surface A horizon of profile TSG0, which correspond to a mean tetrahedral charge of 0.37, 0.35 and 0.24, respectively, per half unit-cell, were observed. The sequence of peaks at 3.69, 1.81 and 1.21 nm indicated a mineral with a mean layer charge of >0.75 per half unit-cell; the intensity of the d_{001} reflection at 3.69 nm exceeded that of the low-charge component (Figure 8). A very small peak was also detected around 2.09 nm, corresponding to a mean layer charge of 0.71 per half unit-cell.

In comparison to the untreated sample, the peak intensity at 3.75 nm in the Li-treated and C18-saturated sample of the surface AE horizon of soil TSG1, corresponding to a mean layer charge of >0.75 per half unit-cell, also increased noticeably. The residual small layer charges of 0.38, 0.33 and 0.22 were denoted by the peaks at 2.11, 1.96 and 1.59 nm, respectively.

In the sample from the E horizon of soil TSG2, two low-charge components were present at 1.86 and 1.61 nm, equivalent to mean layer charges of 0.30 and 0.23. In the AE horizon of soil TSG3, three components were present at 2.03, 1.79 and 1.69 nm, corresponding to clay minerals with mean layer charges of 0.35, 0.28 and 0.23 per half unit-cell, respectively. In this last sample, the reduction of the intensity of the peaks relative to low charge components was less pronounced.

DISCUSSION

Several investigations have shown that in a European Alpine environment, weathering of Podzols leads to a progressive transformation of clay mineral structures, where Al^{3+} and Fe^{3+} substitute for Mg^{2+} in the octahedral sheet. As determined by the common procedure of EG solvation of the clays, the main clay mineral weathering process, which leads to the formation of Podzols, is the appearance of expandable minerals in the surface eluvial horizon. In this study, that process was more evident in the soils developing at middle altitudes, where the combination of rainfall and temperature and the presence of low molecular weight organic acids determine the removal of Fe and Al polymers from the interlayers of expandable minerals (Mirabella and Sartori, 1998; Lundström *et al.*, 2000b; Egli *et al.*, 2001b). A smaller amount of smectitic components could also develop at higher altitudes, but no such minerals were detected in the soil at the lowest elevation. Smectitic components could be the end-product of chlorite or mica weathering or both. It is likely that smectite derives from chlorite, through the removal of hydroxy polymers, whereas mica weathers in a first step to regularly or irregularly interstratified mica-vermiculite clay minerals (Egli *et al.*, 2001b; Mirabella *et al.*, 2002).

Citrate treatment produced some distinctive changes in the XRD patterns of the EG-solvated samples. This procedure allowed the detection of smectitic components in the Bhs or Bs horizons. In particular, the reduction of the charge of clay minerals takes place in those horizons where hydroxy polymers hinder the detection of expandable minerals with the usual ethylene glycol or glycerol solvation procedure (Barnhisel and Bertsch, 1989; Karathanasis, 1988) without any previous treatment that uses a complexing agent. The reduction of the charge of 2:1 clay minerals is a process that occurred before the removal of hydroxy polymers by fulvic acids and low-weight organic acids. This was indicated by citrate treatment where a higher proportion of 2:1 minerals expanded after EG solvation. Due to the more intense podzolization process near the tree line, vermiculites and smectites of the surface-soil horizons usually contained few or no hydroxy interlayers. The site at the lowest altitude and with the lowest susceptibility to weathering therefore had the largest amount of HIV.

Analysis of the d_{060} region showed a temporal evolution of trioctahedral to dioctahedral mineral structures in the well developed Podzols. In the other soils, such a trend was less obvious. This evolution confirms the previously discussed results which show that the soils TSG2 and TSG3 are the most weathered.

The pedogenic smectites from the E or Bhs horizons generally included one or several populations with various interlayer charges, in accord with the results of Righi *et al.* (1997), Gillot *et al.* (2000) and Gillot *et al.* (2001). The heterogeneity is related to the nature of their precursors (Gillot *et al.*, 2000). The layer charges seem to decrease with increasing eluviation of Fe and Al. The soils TSG2 and TSG3, developing near the tree line where the podzolization processes were most intense, had two main charge components. One component had a high charge >0.75 (representing vermiculite-like minerals) and the other had a very low charge near 0.25 (representing smectite). The soils at a higher altitude also had smectites with mean layer charges between 0.35 and 0.41. Aluminous phyllosilicate precursors (phengite, muscovite), being more resistant, would contribute to maintaining higher charge smectites in the sample (Gillot *et al.*, 2001). In most cases, smectite was a heterogeneous mixture of montmorillonite and interstratified beidellite-montmorillonite. A pure beidellite phase could not be detected. The low charges of the beidellitic

https://doi.org/10.1346/CCMN.2003.0510303 Published online by Cambridge University Press

component and montmorillonite were similar because no evident shift of the corresponding peaks was observable in the XRD patterns of C18-saturated samples before and after Li treatment. In fact, the charge obtained with C18-saturated samples (after Li treatment) corresponds only to the beidellitic components, because Li enters into the octahedral sheets of montmorillonite and transforms it into a pyrophyllite-like, uncharged mineral. The interpretation of the Greene-Kelly results might be hampered by several difficulties, because HIV, vermiculite, interstratified mica-vermiculite (or -HIV) could also contribute to the peak at 1.0 nm after Li saturation and heating. The C18 treatment allowed the distinction of two different populations characterized by a low charge in our samples. The intensity of the peaks of the low-charge components decreased when the C18 intercalation was performed on the Li-saturated and heated samples, when compared to the XRD patterns of the C18-saturated but Li-untreated samples. This indicates unambiguously the presence of montmorillonite. Smectites in the eluvial E horizons have been reported as beidellitic in character (Ross and Mortland, 1966; McDaniel *et al*., 1995). According to Gillot *et al*. (2001), smectites having a longer effective time of pedogenesis show lower layer charges. This means that a higher soil weathering state in Podzols leads to smectites with a lower layer charge. This concept is, therefore, also applicable to the climosequence investigated here, where the highest weathering state could be observed in the sites near the tree line (TSG2 and TSG3).

CONCLUSIONS

Climate has noticeably influenced the alteration of clay minerals in the soils studied, leading to the formation of expandable clay minerals with various charges in the surface horizon, with the exception of the soil developing at the lowest altitude.

The origin of smectites could be traced back to chlorite, following removal of hydroxy polymers or to mica, that transforms in a first step to regularly or irregularly interstratified minerals.

More intense weathering of clay minerals was detected in the Podzols at 1600–1800 m a.s.l. which are close to the tree line, where the evolution of trioctahedral to dioctahedral mineral structures was more evident.

The charge reduction of the precursor clay minerals such as mica and chlorite also took place in the Bhs and Bs horizons where the smectites were predominantly hydroxy interlayered. Therefore, the process of charge reduction occurred prior to the removal of hydroxy polymers from the interlayer space of the minerals, the next step in the weathering sequence (seen in the E, AE or A horizons).

The smectite population in the E, AE or A horizons contained different proportions of montmorillonite and interstratified beidellite-montmorillonite, characterized by similar, low layer charges. Generally, lower layer charges were observed in the soils with a higher degree of weathering.

ACKNOWLEDGMENTS

We would like to express our appreciation to Juri Zani for assistance in preparing and performing the XRD procedures. Furthermore, we are indebted to Dr D. Righi and an unknown reviewer for their helpful comments on an earlier version of the manuscript.

REFERENCES

April, R.H., Hluchy, M.M. and Newton, R.M. (1986) The nature of vermiculite in Adirondack soils and till. *Clays and Clay Minerals*, **34**, 549–556.

Barnhisel, R.I. and Bertsch, P.M. (1989) Chlorites and hydroxy-interlayered vermiculite and smectite. Pp. 729–788 in: *Minerals in Soil Environments* 2nd edition (J.B. Dixon and S.B. Weed, editors). Soil Science Society of America, Madison, Wisconsin.

Baroni, C. and Carton, A. (1990) Variazioni oloceniche della Vedretta della Lobbia (gruppo dell'Adamello, Alpi Centrali). *Geografia Fisica Dinamica Quaternaria*, **13**, 105–119.

Carnicelli, S., Mirabella, A., Cecchini, G. and Sanesi, G. (1997) Weathering of chlorite to a low-charge expandable mineral in a Spodosol on the Apennine mountains, Italy. *Clays and Clay Minerals*, **45**, 28–41.

Egli, M., Mirabella, A. and Fitze, P. (2001a) Weathering and evolution of soils formed on granitic, glacial deposits: results from chronosequences of Swiss Alpine environments. *Catena*, **45**, 19–47.

Egli, M., Mirabella, A. and Fitze, P. (2001b) Clay mineral formation in soils of two different chronosequences in the Swiss Alps. *Geoderma*, **104**, 145–175.

Egli, M., Mirabella, A., Sartori, G. and Fitze, P. (2003) Weathering rates as a function of climate: results from a climosequence of the Val Genova (Trentino, Italian Alps). *Geoderma*, **111**, 99–121.

Fanning, D.S., Keramidas, V.Z. and El-Desoky, M.A. (1989) Micas. Pp. 551–634 in: *Minerals in Soil Environments* 2nd edition (J.B. Dixon and S.B. Weed, editors). Soil Science Society of America, Madison, Wisconsin.

FAO-UNESCO (1990) *Soil Map of the World - Revised Legend*. Rome, Italy.

Gillot, F., Righi, D. and Elsass, F. (2000) Pedogenic smectites in Podzols from central Finland: an analytical electron microscopy study. *Clays and Clay Minerals*, **48**, 655–664.

Gillot, F., Righi, D. and Räisänen, M.L. (2001) Layer charge evaluation of expandable clays from a chronosequence of podzols in Finland using an alkylammonium method. *Clay Minerals*, **36**, 571–584.

Greene-Kelly, R. (1953) The identification of montmorillonoids in clays. *Journal of Soil Science*, **4**, 233–237.

Karathanasis, A.D. (1988) Compositional and solubility relationships between aluminum-hydroxy interlayered soil-smectites and vermiculites. *Soil Science Society of America Journal*, **52**, 1500–1508.

Keller, W., Wohlgemuth, T., Kuhn, N., Schütz, M. and Wildi, O. (1998) *Waldgesellschaften der Schweiz auf floristischer Grundlage. Statistisch überarbeitete Fassung der 'Waldgesellschaften und Waldstandorte der Schweiz' von Heinz Elleneberg und Frank Klötzli (1972).* Mitteilungen der Eidgenössischen Forschungsanstalt für Wald, Schnee und Landschaft, Bd. 73, Birmensdorf, Germany.

Lagaly, G. (1994) Layer charge determination by alkylammonium ions. Pp. 1–46 in: *Layer Charge Characteristics of 2:1 Silicate Clay Minerals* (A.R. Mermut, editor). CMS Workshop lectures, **6**. The Clay Minerals Society, Bloomington, Indiana.

Lanson, B. (1997) Decomposition of experimental X-ray diffraction patterns (profile fitting): a convenient way to study clay minerals. *Clays and Clay Minerals* **45**, 132–146.

Lundström, U.S., van Breemen, N. and Bain, D.C. (2000a) The podzolization process. A review. *Geoderma*, **94**, 91–107.

Lundström, U.S., van Breemen, N., Bain, D.C., van Hees, P.A.W., Giesler, R., Gustafsson, J.P., Ilvesniemi, H., Karltun, E., Melkerud, P.-A., Olsson, M., Riise, G., Wahlberg, O., Bergelin, A., Bishop, K., Finlay, R., Jongmans, A.G., Magnusson, T., Mannerkosky, H., Nordgren, A., Nyberg, L., Starr, M. and Tau Strand, L. (2000b) Advances in understanding the podzolization process resulting from a multidisciplinary study of three coniferous forest soils in the Nordic Countries. *Geoderma*, **94**, 335–353.

Malcolm, R.L., Nettleton, W.D. and McCracken, R.J. (1969) Pedogenic formation of montmorillonite from a 2:1–2:2 intergrade clay mineral. *Clays and Clay Minerals*, **16**, 405–414.

McDaniel, P.A., Falen, A.L., Tice, K.R., Graham, R.C. and Fendorf, S.E. (1995) Beidellite in E horizons of northern Idaho Spodosols formed in volcanic ash. *Clays Clay Minerals*, **43**, 525–532.

Melkerud, P.-A., Bain, D.C., Jongmans, A.G. and Tarvainen, T. (2000) Chemical, mineralogical and morphological characterization of three podzols developed on glacial deposits in Northern Europe. *Geoderma*, **94**, 125–148.

Mirabella, A. and Sartori, G. (1998) The effect of climate on the mineralogical properties of soils from the Val Genova Valley (Trentino, Italy). *Fresenius Environmental Bulletin*, **7**, 478–483.

Mirabella, A., Egli, M., Carnicelli, S. and Sartori, G. (2002) Influence of parent material on clay minerals formation in podzols of Trentino – Italy. *Clay Minerals*, **36**, 699–707.

Moore, D.M. and Reynolds, R.C., Jr (1997) X-*ray Diffraction and the Identification and Analysis of Clay Minerals*, 2nd edition. Oxford University Press, New York.

Olis, A.C., Malla, P.B. and Douglas, L.A. (1990) The rapid estimation of the layer charges of 2:1 expanding clays from a single alkylammonium ion expansion. *Clay Minerals*, **25**, 39–50.

Pedrotti, F. (1993) Saggio di carta delle vegetazione della Regione Trentino. *Alto Adige. Bolletino Associazione Italiana di Cartografia*, **87–89**, 149–154.

Petit, S., Caillaud, J., Righi, D., Madejová, J., Elsass, F. and Köster, H.M. (2002) Characterization and crystal chemistry of Fe-rich montmorillonite from Ölberg, Germany. *Clay Minerals*, **37**, 283–297.

Righi, D. and Meunier, A. (1991) Characterization and genetic interpretation of clays in acid brown soil (Dystrochrept) developed in a granitic saprolite. *Clays and Clay Minerals*, **39**, 519–530.

Righi, D., Petit, S. and Bouchet, A. (1993) Characterization of hydroxy-interlayered vermiculite and illite-smectite interstratified minerals from the weathering of chlorite in a Cryorthod. *Clays and Clay Minerals*, **41**, 484–495.

Righi, D., Räisänen, M.L. and Gillot, F. (1997) Clay mineral transformations in podzolized tills in central Finland. *Clay Minerals*, **32**, 531–544.

Righi, D., Huber, K. and Keller, C. (1999) Clay formation and podzol development from postglacial moraines in Switzerland. *Clay Minerals*, **34**, 319–332.

Ross, G.J. (1980) The mineralogy of Spodosols. Pp. 127–143 in: *Soils with Variable Charge* (B.K.G. Theng, editor). Soil Bureau, Department of Scientific and Industrial Research, Lower Hutt, New Zealand.

Ross, G.J. and Mortland, M.M. (1966) A soil beidellite. *Soil Science Society of America Proceedings*, **3**, 337–343.

Sartori, G. and Mancabelli, A. (2002) Atlante dei suoli del Parco Adamello-Brenta. Suoli e paesaggi. *Parco Documenti, Strembo (Trento)*, in press.

Senkayi, A.L., Dixon, J.B. and Hossner, L.R. (1981) Transformation of chlorite to smectite through regularly interstratified intermediates. *Soil Science Society of America Journal*, **45**, 650–656.

Tamura, T. (1958) Identification of clay minerals from acid soils. *Journal of Soil Science*, **9**, 141–147.

Wilson, M.J. (1986) Mineral weathering processes in podzolic soils on granitic materials and their implications for surface water acidification. *Journal of the Geological Society, London*, **143**, 691–697.

(*Received 1 August 2002; revised 6 February 2003; Ms. 703*)